Published in final edited form as:
Ultrasound Med Biol. 2014 April ; 40(4): 755–764. doi:10.1016/j.ultrasmedbio.2013.11.002.

Ultrasound-stimulated drug delivery for treatment of residual disease following incomplete resection of head and neck cancer

Anna G. Sorace[1,2], **Melissa Korb**[3], **Jason M. Warram**[2], **Heidi Umphrey**[2,5], **Kurt R. Zinn**[1,2,4,5], **Eben Rosenthal**[3,5], and **Kenneth Hoyt**[1,2,4,5]

[1]Department of Biomedical Engineering, 1530 3rd Avenue South, Box 601, University of Alabama at Birmingham, Birmingham, AL 35294-0019

[2]Department of Radiology, 1530 3rd Avenue South, Box 601, University of Alabama at Birmingham, Birmingham, AL 35294-0019

[3]Department of Surgery, 1530 3rd Avenue South, Box 601, University of Alabama at Birmingham, Birmingham, AL 35294-0019

[4]Department of Electrical & Computer Engineering, 1530 3rd Avenue South, Box 601, University of Alabama at Birmingham, Birmingham, AL 35294-0019

[5]Comprehensive Cancer Center, 1530 3rd Avenue South, Box 601, University of Alabama at Birmingham, Birmingham, AL 35294-0019

Abstract

Microbubbles triggered with localized ultrasound (US) can improve tumor drug delivery and retention. Termed US-stimulated drug delivery, this strategy was applied to head and neck cancer (HNC) in a post-surgical tumor resection model. Nude athymic mice (N = 24) were implanted in the flank with luciferase-positive HNC squamous cell carcinoma (SCC) and underwent various degrees of surgical tumor resection (0%, 50% or 100%). Following surgery, animals received adjuvant therapy with cetuximab-IRDye alone, cetuximab-IRDye in combination with US-stimulated drug delivery, or saline injections (control) on days 4, 7, and 10. Tumor drug delivery was assessed on days 0, 4, 7, 10, 14, and 17 with an *in vivo* fluorescence imaging system, while tumor viability was evaluated at the same time points with *in vivo* bioluminescence imaging. Tumor caliper measurements occurred two times per week for days. Optical imaging demonstrated that in the 50% tumor resection group, US-stimulated drug delivery resulted in a significant increase in cetuximab delivery compared to drug alone on day 10 (day of peak fluorescence) (p = 0.03). Tumor viability decreased in all groups receiving US-stimulated drug delivery plus drug compared to the drug alone group. After various degrees of surgical resection, this novel study demonstrates positive improvements in drug uptake in the residual cancer cells when combined with US-stimulated drug delivery.

Corresponding author: Kenneth Hoyt, PhD, MBA, G082 Volker Hall, 1530 3rd Ave S, Birmingham, AL 35294-0019, Ph: (205) 934-3116, Fx: (205) 975-6522, hoyt@uab.edu.

Keywords

adjuvant therapy; cetuximab; drug delivery; head and neck cancer; microbubbles; optical imaging; ultrasound

INTRODUCTION

Tumor retention and vascular permeability can be reversibly enhanced using mechanically oscillating microbubble (MB) contrast agents exposed to a low-intensity ultrasound (US) field in a process known as US-stimulated drug delivery. This strategy was first introduced to augment delivery of molecules through the blood-brain barrier (Hynynen, McDannold 2003, Marty, Larrat 2012, McDannold, Arvanitis 2012, Schlachetzki, Hölscher 2002), and has since been investigated for multiple other purposes. This transient increase in membrane permeability introduces a therapeutic window where enhanced drug uptake occurs, thereby improving the anticancer effects. This relatively noninvasive approach to cancer treatment is generally considered non-toxic, safe, and effective. US-stimulated drug delivery has demonstrated a 20 to 80% improvement in tumor response to drug treatment compared to drug alone in preclinical murine models (Bekeredjian, Kroll 2007, Casey, Cashman 2010, Heath, Sorace 2012, Iwanaga, Tominaga 2007, Park, Zhang 2012, Sorace, Warram 2012). To improve therapeutic effectiveness, novel treatment strategies are needed to overcome the current barriers of poor drug uptake resulting from tortuous vasculature, limited drug dosages and high tumor interstitial pressure (Jain and Carmeliet 2012, Jain and Carmeliet 2001). Preclinical *in vivo* cancer research traditionally evaluates treatments through a neoadjuvant animal model by treating primary solid tumors. To date, research in the US-stimulated drug delivery field for cancer treatment has focused on improving localized delivery of molecules, such as drugs, DNA, or virus (Dalecki 2004, Escoffre, Piron 2011, Kinoshita, McDannold 2006, Lentacker, Vandenbroucke 2008).

In most cancer types, including head and neck cancer (HNC), treatment strategies involve surgery followed by chemotherapy or radiation. Residual disease is common in HNC and systemic therapy is delivered to further regress tumor size or treat margins that were unable to be surgically resected (Vermorken and Specenier 2010). Currently, HNC patients who undergo surgical resection of a localized tumor have an 80% likelihood of disease recurrence within two years (Ridge, Mehra 2013). To improve overall HNC patient survival, it is critical to improve delivery of adjuvant therapy to any residual disease to help improve the therapeutic outcome and reduce cancer reoccurrence. The devascularized wound bed remaining after surgical removal of a tumor can hinder drug extravasation, thereby further heightening the difficulty of systemic adjuvant treatment.

US-stimulated drug delivery has the potential to improve adjuvant chemotherapy delivery to residual disease and reduce recurrence in HNC. The effectiveness of a therapeutic drug is directly dependent upon the amount delivered to the tumor. In this paper, we investigate the effects of US-stimulated drug delivery on residual disease in a preclinical animal model of HNC. The model system detailed provides the basis for advancing preclinical surgical models of adjuvant US-stimulated drug delivery in various cancer types with a range of chemotherapeutics. Findings from this study may help advance US-stimulated drug delivery towards clinical translational.

MATERIALS AND METHODS

Cell preparation

Luciferase-positive HNC cells (squamous cell carcinoma (SCC) 1, provided by Thomas Carey, PhD, University of Michigan, Ann Arbor, MI) were maintained in DMEM media, supplemented with 10% Fetal Bovine Serum and 1% L-glutamate. Cells were passaged at 90% confluency and stored at 37°C and 5% CO_2. Cell counts and viability was determined through hemocytometry and trypan blue dye exclusion.

Animal care and tumor implants

All animal work was reviewed and approved by the Institute of Animal Care and Use Committee at the University of Alabama at Birmingham. Tumor implantation used a 27.5 gauge needle and injected 2×10^6 cells/100μl DMEM media (without FBS) subcutaneously into the right flank of five-week-old female nude athymic mice (Jackson Laboratory, Bar Harbor, ME) (N=24). Tumor growth was measured biweekly until day 24 using calipers. Given basic tumor diameter measurements along the transverse d_t and longitudinal d_l dimensions, tumor size was calculated using the equation: $\pi \times (d_t/2) \times (d_l/2)$. These caliper measurements reflect tumor size and do not account for necrotic or apoptotic regions.

Surgical resection

Mice were sorted into nine groups: surgical resection (0%, 50%, or 100%) + US + drug, surgical resection (0%, 50%, or 100%) + drug, or surgical resection (0%, 50%, or 100%) alone (N = 3 for surgical resection + US + drug and surgical resection + drug groups, N = 2 for surgical resection control group). The average tumor size for each group was approximately equal (18.7 ± 1.9 mm^2 at day 0). Prior to surgery, mice underwent baseline imaging and tumor caliper measurements. Mice underwent surgical removal of the tumor at 0% resection (no tumor was removed; sham surgery was administered), 50% resection (50% of the tumor remained), and 100% resection (surgeon removed 100% of the tumor noted by visualization and palpation). Regardless of the groups, all mice underwent identical surgical procedures. Briefly, a surgical blade (Feather 2976 #15, Osaka, Japan) was used to open a flap of skin in an “L” shape, leaving an estimated one centimeter of space around the tumor. The skin flap was sharply dissected from the surface of the tumor and the tumor was then removed at 0%, 50%, or 100% with respect to its designated group. A licensed surgical resident performed each tumor resection. Suturing was completed with 6-0 fast absorbing plain gut suture using a PC-1 conventional cutting 3/8 circle needle (1916, Ethicon, San Angelo, TX). After the wound was closed, mice were subcutaneously injected near the incision site with a 100 μg cocktail of 1 mg/mL Carprofen and 20 μg/mL of Buprenorphine to help relieve any residual pain from surgery. A surgical outline of events is detailed with images in Figure 1. Mice were allowed to heal for four days before follow-up experimental studies began.

Cetuximab-IRDye

Cetuximab was labeled with near-infrared IRDye at the UAB Vector Production Facility according to Current Good Manufacturing Practices. This conjugation resulted in 1.8 IRDye molecules per cetuximab molecule. Cetuximab is a monoclonal antibody targeted to the epidermal growth factor receptor (EGFR) and has been FDA approved for treating HNC as a single agent therapy.

Ultrasound-stimulated drug delivery

US-stimulated drug delivery was applied for 5 min using a 1.0 MHz single element (19 mm diameter) unfocused immersion transducer (Olympus, Waltham, MA) placed 4 cm from the

tumor and the following US exposure parameters: peak negative pressure of 0.9 MPa, pulse repetition period of 15 sec, and a 5% duty cycle. The transducer was in series with a signal generator (AFG3022B, Tektronix, Beaverton, OR) and power amplifier (A075, Electronics and Innovation, Rochester, NY). The unfocused transducer allowed the entire tumor to be exposed to US energy concurrently. For the group of mice to receive US-stimulated cetuximab delivery, a 30 μL dose of MB contrast agent (Definity, Lantheus Medical Imaging, North Billerica, MA) was injected systemically via the tail vein in combination with 200 μg (100 μL) of Cetuximab-IRDye. The drug alone group received 200 μg (100 μL) of Cetuximab-IRDye only while control group mice received 100 μL saline injections. Following a two minute period to allow for adequate systemic circulation of MBs, mice were submerged in a custom-built 37°C water bath and remained under isoflurane gas anesthesia for the entirety of the US-based treatment session. Control mice received sham US exposure. US-stimulated drug delivery occurred on days 4, 7, and 10.

Bioluminescence imaging

Bioluminescence imaging occurred on days 0 (both pre and post-surgery), 4, 7, 10, 14, and 17. Mice were injected intraperitoneal with firefly luciferin (2.5 mg). After a 15 min delay for systemic circulation, all mice were imaged for bioluminescence expression using a small animal imaging system (IVIS-100, Xenogen, BioSciences, Cranbury, NJ, USA). All mice were imaged in the prone position (dorsal side up). Five mice were imaged per time sequence using a 1 sec exposure, an f/stop of 1, binning of 8, and at 25 cm camera distance. A low exposure time was required to eliminate oversaturation of the optical signal. A standardized circular region-of-interest (ROI) was placed around each mouse tumor and the total photon counts were quantified within the region.

Fluorescence imaging

Fluorescence imaging was completed on days 0, 4, 7, 10, 14, 17. On days that imaging coincided with US-stimulated drug delivery, optical imaging took place at least one hour post therapy using a dedicated small animal optical imaging system (Pearl Impulse, LI-COR Biotechnology, Lincoln, NE). Imaging was performed using the near-infrared 800-nm channel, exciting at a wavelength of 778 nm and detected at 794 nm. Animals were maintained under isoflurane anesthesia and were prone positioned. Using commercial software (Pearl Impulse Software Version 2.0, LI-COR Biotechnology), an ROI was manually drawn around each tumor in the fluorescence image given a co-registered digital photograph for guidance. This was done separately for each image, as there are slight differences in mouse positioning and tumor size. If there was a complete tumor resection and no tumor was present when imaged, an ROI was drawn approximately around the area of tumor removal. Total fluorescence signal intensity within that ROI was measured and normalized by total pixel counts to quantify mean tumor fluorescence.

Survival analysis

Survival analysis was performed for 60 days after surgery. If a tumor exceeded IACUC standards for size, exhibited signs of ulceration, or if the animal became sick or distressed, the animal was humanely euthanized and that day was recorded as the terminal date. Tumors that were completely resected were also monitored for regrowth. A complete timeline of the experimental design is detailed in Figure 2.

Statistical analysis

All experimental data was summarized as mean ± SE. An analysis of variance (ANOVA) test was used to assess differences within the different group data. A paired *t*-test was used to compare the initial baseline bioluminescence image measurements with their subsequent

values at day 17. This was also completed between baseline and day 10 using the fluorescence imaging data. A *p*-value of less than 0.05 was considered statistically significant. All analyses were completed using statistical software (SAS 9.2, SAS Institute Inc, Cary, NC, USA).

RESULTS

Control group mice, overall, exhibited an increase in tumor size compared to groups receiving therapy (US-stimulated drug delivery or drug alone, $p < 0.04$). As detailed in Figure 3 for the 0% tumor resection control group, caliper measurements revealed a 67.8 mm^2 increase in tumor growth over baseline (day 0) at day 24. Also, the 50% tumor resection control group had a 18.3 mm^2 increase at day 24 compared to baseline measures (post-surgery) while the 100% resection group showed a 6.57 mm^2 increase.

Bioluminescence imaging was employed to quantify viable cancer cells within a given tumor region. Comparing pre- and post-surgery tumor viability on day 0 revealed that the 0% tumor resection group demonstrated no change following sham surgery. Conversely, bioluminescence from the 50% tumor resection group was shown to be decreased by 77% and the 100% complete tumor resection revealed a 99% decrease in viable tumor burden. After an initial analysis of tumor reduction following surgery, residual tumors were tracked individually as percent change from their post-surgical state. Each of the control groups (no drugs administered) produced an overall increase in bioluminescence signals following tumor removal (day 0) to day 17; 0% resection, 50% resection, and 100% resection revealed a 2-fold, 3071-fold, and a 701-fold increase, respectively. Control data exhibited a pronounced exponential increase over the drug alone and US-stimulated drug delivery group bioluminescence signal measurements. Compared to mice that received drug alone, at day 17, mice subjected to US-stimulated drug delivery resulted in a 2-fold decrease in bioluminescence signal measures (viable tumor) for the 0% tumor resection group (Figure 4a), 66-fold decrease in the 50% tumor resection group (Figure 4b), and a 2.6-fold decrease in the 100% tumor resection group (Figure 4c). For the mice that received repeated sessions of US-stimulated drug delivery, the 0% and the 100% tumor resection mice groups exhibited an overall decrease by day 17 in tumor viability compared to the initial post-surgery baseline imaging. Bioluminescence data collected from the 50% tumor resection group mice revealed an increase in viability on day 17. A decrease in percent change of bioluminescence signal indicates that there is less viable tissue than the baseline measurements, indicating cell death.

Fluorescence imaging was used to monitor delivery of the IR-labeled drug and more specifically to determine if US-stimulated drug delivery enhances tumor uptake and retention of the therapeutic agent. Figure 5 suggests that the greatest enhancement of drug uptake occurred on day 10 according to peak fluorescence image measurements. All surgical group mice receiving US-stimulated drug delivery showed a significant increase in tumor fluorescence compared to control tumors that received sham US therapy ($p < 0.04$). Mice tumors that did not undergo surgical resection but received US-stimulated drug delivery exhibited a mean fluorescence signal increase of 42.3% on day 10 when compared to mice subjected to systemic drug treatment only ($p = 0.10$). Also at day 10 post-surgery, tumors that underwent a partial 50% resection and subjected to US-stimulated drug delivery demonstrated a 41.6% increase in fluorescence measurements compared to residual disease treated with drug only ($p = 0.03$). Lastly, a comparison of day 10 fluorescence imaging results from groups that received US-stimulated drug delivery versus drug following surgical resection of the entire tumor revealed no significant changes in fluorescent signal in the remaining wound bed ($p = 0.48$). On day 17 of fluorescence imaging, all of these trends continued, however the signal from the tumors was markedly decreased.

All mice in the 50% and 100% tumor resection groups showed complete survival over the 60 day study. For the 0% tumor resection group mice, none of the control animals remained on day 36. However, all of the mice subjected to drug treatment alone or US-stimulated drug delivery survived. For tumors that were completely (100%) resected, both the control and drug only dosed mice had a 66% reoccurrence rate of disease, while the US-stimulated drug delivery group improved treatment of any residual disease and importantly no tumor reoccurrence was observed.

DISCUSSION

Many cancer-fighting therapies have shown strong antitumor effects in preclinical models of primary tumors but fail to translate clinically for prevention of disease recurrence after surgery (Block, Nevala 2011, Grinshtein, Bridle 2009, Schreiber, Rowley 2006, Tucker, Laguna 2012). Surgery promotes inhibitory factors that allow lingering immunosuppressive cells to repopulate minute pockets of residual disease quickly (Predina, Eruslanov 2013). This system of immunosuppression in the post-surgical tumor microenvironment explains the resistance of cancer to conventional therapies despite its small residual volume (Predina, Eruslanov 2013). Surgery has also shown to have no impact on the alterations of remaining cells or their resistance to drugs (Predina, Eruslanov 2013). HNC treatment consisting of surgical resection and adjuvant therapy is generally considered effective; however, many of these cases result in cancer recurrence due to residual viable cancer cells left behind after surgery. This is partially due to vital internal structures that cannot be damaged/removed or incomplete visualization of the tumor. Notwithstanding, the devascularized wound bed following surgical removal of a tumorous mass leaves a difficult environment for treatment. US-stimulated drug delivery has been explored in numerous preclinical animal studies for improving drug delivery to solid tumors in the neoadjuvant setting. We believe that exploration of combination treatment with surgical resection is a necessity to advance this research towards clinical translation. In this paper, we evaluated the benefit of applying US-stimulated drug delivery to HNC-bearing mice that underwent surgical resection of the primary tumor burden. The use of a multimodality imaging strategy allowed discrimination of improved drug uptake in the target tumor in response to US-stimulated drug delivery and viability of any residual tumor (disease).

EGFR is overexpressed in many solid tumors, including SCC of the head and neck (Masui, Kawamoto 1984). High expression of EGFR is linked to poor prognosis after treatment; therefore it is an excellent target for treating this disease (Haddad and Shin 2008). EGFR is a transmembrane protein with intrinsic tyrosine kinase activity that regulates cell growth in response to binding of its ligands, such as epidermal growth factor (EGF) and transforming growth factor α (TGF-α) (Ang, Berkey 2002, Rubin Grandis, Melhem 1998). Ligand binding induces EGFR dimerization and activates several EGFR-mediated signaling pathways. In order for cetuximab to properly operate, it has to bind to the proper receptor to begin the cascade pathway. Due to the immense treatment potential, clinical studies have been ongoing for the last decades analyzing EGFR targeted-based therapies. While cetuximab is not currently approved for use in adjuvant therapy, it is currently being explored in clinical trials. A phase II trial demonstrated superior cancer control at one year when using cetuximab in combination with radiotherapy, than radiotherapy alone (Mesía, Rueda 2013). Adjuvant cetuximab is also being explored with either cisplatin or docetaxel in Stage III and IV SCC patients (Harari, Kies 2011). Additionally, there are other targeted EGFR agents that have moved forward to be used as adjuvant therapies. In SCC of the HNC, there is recruitment for a phase III trial studying the effects of lapatinib (an EGFR-targeted antibody) in patients following surgery. Clinical studies analyzing the effects of trastuzumab (monoclonal antibody against the human epidermal growth factor receptor 2, HER2) in combination with traditional chemotherapies as an adjuvant therapy have now

become standard-of-care in breast cancer. The addition of this targeted antibody revealed a significant increase in anticancer effects and survival (Perez, Romond 2011). With promising results in both preclinical and clinical trials using EGFR-targeted antibodies, there is an expanding amount of clinical research ongoing for these monoclonal antibodies as single therapies, as well as in combination with traditional chemotherapy (Moon, Chae 2010). Research has shown that targeted therapies can improve antitumor effects post-surgery; therefore, further heightening tumor retention and delivery through non-invasive methods would be a valuable addition to current methods of treatment.

Studies have shown that intravascular MB contrast agents exposed to US energy can increase extravasation by breaking down gap junctions between endothelial cells allowing transport of molecules across barriers that previously would be unable to cross (Caskey, Stieger 2007, Chen, Kreider 2011, Miller, Pislaru 2002, Zderic, Vaezy 2002, Zhao, Dai 2012). This unique therapy has been applied to many disease types and for modulating delivery of a host of molecular agents. A previous study has shown that tumors subjected to US-stimulated drug delivery using cetuximab exhibited significantly increased antitumor effects compared to drug alone when analyzing tumor size (Heath, Sorace 2012). These effects were confirmed by both immunohistologic analysis and diffusion-weighted magnetic resonance imaging (DW-MRI), demonstrating a 20% increase in apparent diffusion coefficient (ADC) values (*i.e.*, increased apoptotic activity and cell death) when comparing tumors treated with US-stimulated drug delivery compared to drug alone. When exploring other *in vivo* applications of US-stimulated drug delivery, previously reported methods analyzed secondary indicators of tumor response to treatment by measuring size and evaluating histological results post-mortem (Zhao, Lu 2011). MRI-based measures have also shown to be effective in confirming US-stimulated drug delivery through the blood-brain barrier (Kinoshita, McDannold 2006, McDannold, Arvanitis 2012, O'Reilly, Waspe 2012, Treat, McDannold 2012). The ability to image at near-infrared fluorescence wavelengths decreases error by minimizing the fluorescence signal contributed from background tissue, allowing for more precise measurements (Frangioni 2003, Hebden, Arridge 1997). Optical imaging of fluorescently-labeled drugs has shown potential for monitoring preclinical molecular delivery in neoadjuvant models (Jiang, Gnanasammandhan 2010), in surgical-resection models (Day, Beck 2013, Heath, Deep 2012), and US-stimulated therapeutic models (Sorace, Saini 2013).

Bioluminescence imaging allows visualization of viable (luciferase-positive) tumor tissue in comparison to the more routine tumor size measurements which cannot differentiate viable from necrotic tissue. In this paper, it was shown that both the 0% and 100% tumor resection mice groups receiving US-stimulated drug delivery exhibited enhanced antitumor activity compared to animals receiving drug alone. This response was highlighted by a progressive decrease in the amount of viable tumor tissue from baseline measures. However, mice that underwent surgery to remove only 50% of the tumor showed an increased antitumor effect compared to drug alone, yet did not regress when compared to baseline values. This was an interesting result, as the tumor viability seemed to grow exponentially quicker in tumors that received partial resection compared to complete or no resection. It is hypothesized that the mouse's innate cell-mediated immune response may have reacted similar to a tissue wound injury and counteractively worked to repair the injured tumor site, thereby increasing cell growth. It is important to note that all three control groups (including the 100% tumor resection group) exhibited an increase in tumor viability and physical size. Surgery alone was not sufficient enough to impede tumor growth. Although caliper measurements are not known for their precision, they demonstrated a consistent trend in that the control group tumor grew exponentially compared to the groups receiving US-stimulated drug delivery or drug alone. Caliper measurements and bioluminescence were utilized in order to assess changes in both tumor size and tumor cell viability. Bioluminescence is considered a more

accurate measurement of response; however tumor sizes are currently used clinically to assess changes in tumor response. A possible reason for variation between bioluminescence and tumor caliper measurements is a portion of the tumor has potential to be coalesced with the skin when measuring with calipers, as well as low numbers have potential to create higher variations within each group. Bioluminescence imaging also has potential for human error through variances in mouse positioning and luciferin injections between days of a longitudinal study. As seen in Figure 3, the caliper measurements alone are not precise enough to determine differences in treated groups. Analysis of fluorescence imaging results from mice that underwent 100% tumor resection revealed that there were no significant differences in drug uptake for tumors treated with US-stimulated drug delivery or drug alone. This is expected as the ROIs during fluorescence monitoring of these data sets may not have had a visible tumor. After a single dose of cetuximab (day 4), no changes in drug uptake (tumor fluorescence) was observed for any of the groups at one hour post-delivery, which is consistent with previous research that looked at immediate uptake of fluorescently-labeled IgG molecules after US-stimulated drug delivery in a primary tumor model (Sorace, Saini 2013). It is believed that multiple doses of US-stimulated drug delivery further enhanced delivery and is essential for delivery of targeted antibodies, as cetuximab has been previously shown to be effective in a multi-dose longitudinal study (Heath, Sorace 2012). However, fluorescence imaging of the 0% and 50% tumor resection model demonstrated heightened drug delivery when systemic injections of cetuximab were supplemented with US-stimulated drug delivery. Day 10 showed the greatest enhancement with a 42% increase in fluorescence signal measurements in the US-stimulated drug delivery group mice compared to those administered drug alone. Fluorescence signal decreases overtime, therefore it is logical that signal peaked on the final day of drug administration. On day 17, there was a significant correlation between percent change in fluorescence and bioluminescence ($R^2 = 0.57$, $p < 0.001$). This allows us to conclude that the drug delivery was correlated to overall tumor viability response. US-stimulated drug delivery enhances localized cetuximab delivery, thereby enhancing tumor response to therapy. High variance found within the groups was due to low group numbers. Although no differences were found with a 60 day survival analysis, disease reoccurrence was observed in the 100% tumor resection group mice that did not receive US-stimulated drug delivery to improve treatment of any residual cancer cells. Due to its high binding efficiency, cetuximab-IRDye has been previously shown to be utilized preclinically to assist in surgical resection of head and neck cancer (Day, Sweeny 2013), as well as for its therapeutic potential (Gleysteen, Duncan 2007). Therefore due to its proven effectiveness in the treatment of head and neck cancer, it was an ideal choice of therapy to administer in this study in order to both treat and monitor drug delivery. Previous studies have also reported that US therapy can significantly improve neoadjuvant cetuximab-IRDye delivery to the tumor through post-mortem histological analysis of the localized fluorescence signal (Sorace 2013). Histological analysis was not completed in this study, as the mice were tracked for survival after completion of therapy.

The overall goal of this novel study was to evaluate this unique therapy in combination with surgical resection. US-stimulated therapy revealed promising results for the treatment of cancer when utilized in combination with surgery and systemic therapy. Utilizing multiple methods, such as tumor measurements, fluorescence, and bioluminescence, this study gave initial results which warrants further exploration into US-stimulated adjuvant therapy in cancers which commonly result in residual disease following surgical resection.

CONCLUSIONS

This study produced encouraging preclinical results exploring the use of US-stimulated drug delivery in the adjuvant setting for the treatment of residual disease following incomplete resection of HNC. Given HNC patients are at a high risk for recurrence of the primary tumor

even after surgical intervention and follow-up drug or radiation treatment, developing methods that will help reduce this disease recurrence is critically important for improving patient prognosis and long-term survival. In conclusion, US-stimulated drug delivery is a promising technology and more research is warranted to explore this technique to improve drug delivery and tumor response to residual disease after surgical resection.

Acknowledgments

This research was supported by grant 1RO1CA142637 from the National Cancer Institute, grant 2T32CA091078-06 from the National Institutes of Health, and through a pilot award from the Department of Radiology at the University of Alabama at Birmingham.

REFERENCES

Ang KK, Berkey BA, Tu X, Zhang HZ, Katz R, Hammond EH, Fu KK, Milas L. Impact of epidermal growth factor receptor expression on survival and pattern of relapse in patients with advanced head and neck carcinoma. Cancer Res. 2002; 62:7350–7356. [PubMed: 12499279]

Bekeredjian R, Kroll RD, Fein E, Tinkov S, Coester C, Winter G, Katus HA, Kulaksiz H. Ultrasound targeted microbubble destruction increases capillary permeability in hepatomas. Ultrasound Med Biol. 2007; 33:1592–1598. [PubMed: 17618040]

Block MS, Nevala WK, Leontovich AA, Markovic SN. Differential response of human and mouse dendritic cells to VEGF determines interspecies discrepancies in tumor-mediated TH1/TH2 polarity shift. Clin Cancer Res. 2011; 17:1776–1783. [PubMed: 21349994]

Casey G, Cashman JP, Morrissey D, Whelan MC, Larkin JO, Soden DM, Tangney M, O'Sullivan GC. Sonoporation mediated immunogene therapy of solid tumors. Ultrasound Med Biol. 2010; 36:430–440. [PubMed: 20133039]

Caskey CF, Stieger SM, Qin S, Dayton PA, Ferrara KW. Direct observations of ultrasound microbubble contrast agent interaction with the microvessel wall. J Acoust Soc Am. 2007; 122:1191–1200. [PubMed: 17672665]

Chen H, Kreider W, Brayman AA, Bailey MR, Matula TJ. Blood vessel deformations on microsecond time scales by ultrasonic cavitation. Phys Rev Lett. 2011; 106:034301. [PubMed: 21405276]

Dalecki D. Mechanical bioeffects of ultrasound. Annu Rev Biomed Eng. 2004; 6:229–248. [PubMed: 15255769]

Day K, Beck L, Deep M, Kovar J, Zinn K, Rosenthal E. Fluorescently labeled therapeutic antibodies for detection of microscopic melanoma. Laryngoscope. 2013 (In press).

Day KE, Sweeny L, Kulbersh B, Zinn KR, Rosenthal EL. Preclinical Comparison of Near-Infrared-Labeled Cetuximab and Panitumumab for Optical Imaging of Head and Neck Squamous Cell Carcinoma. Mol Imaging Biol. 2013 (In press).

Escoffre JM, Piron J, Novell A, Bouakaz A. Doxorubicin delivery into tumor cells with ultrasound and microbubbles. Mol Pharm. 2011; 8:799–806. [PubMed: 21495672]

Frangioni JV. In vivo near-infrared fluorescence imaging. Curr Opin Chem Biol. 2003; 7:626–634. [PubMed: 14580568]

Gleysteen JP, Duncan RD, Magnuson JS, Skipper JB, Zinn K, Rosenthal EL. Fluorescently labeled cetuximab to evaluate head and neck cancer response to treatment. Cancer Biol Ther. 2007; 6:1181–1185. [PubMed: 17637562]

Grinshtein N, Bridle B, Wan Y, Bramson JL. Neoadjuvant vaccination provides superior protection against tumor relapse following surgery compared with adjuvant vaccination. Cancer Res. 2009; 69:3979–3985. [PubMed: 19383917]

Haddad RI, Shin DM. Recent advances in head and neck cancer. N Engl J Med. 2008; 359:1143–1154. [PubMed: 18784104]

Harari, P.; Kies, MS.; Myers, JN. Adjuvant Cetuximab and Chemoradiotherapy Using Either Cisplatin or Docetaxel in Treating Patients With Resected Stage III or Stage IV Squamous Cell Carcinoma or Lymphoepithelioma of the Head and Neck. National Cancer Institute: Radiation Therapy Oncology Group; 2011. Clinical Trials.gov NCT00084318:

Heath CH, Deep NL, Sweeny L, Zinn KR, Rosenthal EL. Use of panitumumab-IRDye800 to image microscopic head and neck cancer in an orthotopic surgical model. Ann Surg Oncol. 2012; 19:3879–3887. [PubMed: 22669455]

Heath CH, Sorace A, Knowles J, Rosenthal E, Hoyt K. Microbubble therapy enhances antitumor properties of cisplatin and cetuximab in vitro and in vivo. Otolaryngol Head Neck Surg. 2012; 146:938–945. [PubMed: 22323435]

Hebden JC, Arridge SR, Delpy DT. Optical imaging in medicine: I. Experimental techniques. Phys Med Biol. 1997; 42:825–840. [PubMed: 9172262]

Hynynen K, McDannold N, Vykhodtseva N, Jolesz FA. Non-invasive opening of BBB by focused ultrasound. Acta Neurochir Suppl. 2003; 86:555–558. [PubMed: 14753505]

Iwanaga K, Tominaga K, Yamamoto K, Habu M, Maeda H, Akifusa S, Tsujisawa T, Okinaga T, Fukuda J, Nishihara T. Local delivery system of cytotoxic agents to tumors by focused sonoporation. Cancer Gene Ther. 2007; 14:354–363. [PubMed: 17273182]

Jain RK, Carmeliet P. SnapShot: Tumor angiogenesis. Cell. 2012; 149 1408-08.e1.

Jain RK, Carmeliet PF. Vessels of death or life. Sci Am. 2001; 285:38–45. [PubMed: 11759584]

Jiang S, Gnanasammandhan MK, Zhang Y. Optical imaging-guided cancer therapy with fluorescent nanoparticles. J R Soc Interface. 2010; 7:3–18. [PubMed: 19759055]

Kinoshita M, McDannold N, Jolesz FA, Hynynen K. Noninvasive localized delivery of Herceptin to the mouse brain by MRI-guided focused ultrasound-induced blood-brain barrier disruption. Proc Natl Acad Sci U S A. 2006; 103:11719–11723. [PubMed: 16868082]

Lentacker I, Vandenbroucke RE, Lucas B, Demeester J, De Smedt SC, Sanders NN. New strategies for nucleic acid delivery to conquer cellular and nuclear membranes. J Control Release. 2008; 132:279–288. [PubMed: 18655814]

Marty B, Larrat B, Van Landeghem M, Robic C, Robert P, Port M, Le Bihan D, Pernot M, Tanter M, Lethimonnier F, Mériaux S. Dynamic study of blood-brain barrier closure after its disruption using ultrasound: a quantitative analysis. J Cereb Blood Flow Metab. 2012; 32:1948–1958. [PubMed: 22805875]

Masui H, Kawamoto T, Sato JD, Wolf B, Sato G, Mendelsohn J. Growth inhibition of human tumor cells in athymic mice by anti-epidermal growth factor receptor monoclonal antibodies. Cancer Res. 1984; 44:1002–1007. [PubMed: 6318979]

McDannold N, Arvanitis CD, Vykhodtseva N, Livingstone MS. Temporary disruption of the blood-brain barrier by use of ultrasound and microbubbles: safety and efficacy evaluation in rhesus macaques. Cancer Res. 2012; 72:3652–3663. [PubMed: 22552291]

Mesía R, Rueda A, Vera R, Lozano A, Medina JA, Aguiar D, Árias F, Triana G, Carles J, López-López R. Adjuvant therapy with cetuximab for locally advanced squamous cell carcinoma of the oropharynx: results from a randomized, phase II prospective trial. Ann Oncol. 2013; 24:448–453. [PubMed: 23041591]

Miller DL, Pislaru SV, Greenleaf JE. Sonoporation: mechanical DNA delivery by ultrasonic cavitation. Somat Cell Mol Genet. 2002; 27:115–134. [PubMed: 12774945]

Moon C, Chae YK, Lee J. Targeting epidermal growth factor receptor in head and neck cancer: lessons learned from cetuximab. Exp Biol Med (Maywood). 2010; 235:907–920. [PubMed: 20562132]

O'Reilly MA, Waspe AC, Chopra R, Hynynen K. MRI-guided disruption of the blood-brain barrier using transcranial focused ultrasound in a rat model. J Vis Exp. 2012

Park EJ, Zhang YZ, Vykhodtseva N, McDannold N. Ultrasound-mediated blood-brain/blood-tumor barrier disruption improves outcomes with trastuzumab in a breast cancer brain metastasis model. J Control Release. 2012; 163:277–284. [PubMed: 23000189]

Perez EA, Romond EH, Suman VJ, Jeong JH, Davidson NE, Geyer CE, Martino S, Mamounas EP, Kaufman PA, Wolmark N. Four-year follow-up of trastuzumab plus adjuvant chemotherapy for operable human epidermal growth factor receptor 2-positive breast cancer: joint analysis of data from NCCTG N9831 and NSABP B-31. J Clin Oncol. 2011; 29:3366–3373. [PubMed: 21768458]

Predina J, Eruslanov E, Judy B, Kapoor V, Cheng G, Wang LC, Sun J, Moon EK, Fridlender ZG, Albelda S, Singhal S. Changes in the local tumor microenvironment in recurrent cancers may explain the failure of vaccines after surgery. Proc Natl Acad Sci U S A. 2013; 110:E415–E424. [PubMed: 23271806]

Ridge JA, Mehra R, Lango MN, Feigenberg S. Head and Neck Tumors. Cancer Management: Cancers of the head and neck region. 2013 Online Edition.

Rubin Grandis J, Melhem MF, Gooding WE, Day R, Holst VA, Wagener MM, Drenning SD, Tweardy DJ. Levels of TGF-alpha and EGFR protein in head and neck squamous cell carcinoma and patient survival. J Natl Cancer Inst. 1998; 90:824–832. [PubMed: 9625170]

Schlachetzki F, Hölscher T, Koch HJ, Draganski B, May A, Schuierer G, Bogdahn U. Observation on the integrity of the blood-brain barrier after microbubble destruction by diagnostic transcranial color-coded sonography. J Ultrasound Med. 2002; 21:419–429. [PubMed: 11934099]

Schreiber K, Rowley DA, Riethmüller G, Schreiber H. Cancer immunotherapy and preclinical studies: why we are not wasting our time with animal experiments. Hematol Oncol Clin North Am. 2006; 20:567–584. [PubMed: 16762725]

Sorace, A. Ph.D. dissertation. University of Alabama at Birmingham; 2013. Microbubble-mediated ultrasound therapy for enhanced drug delivery in cancer.

Sorace AG, Saini R, Rosenthal E, Warram JM, Zinn KR, Hoyt K. Optical fluorescent imaging to monitor temporal effects of microbubble-mediated ultrasound therapy. IEEE Trans Ultrason Ferroelectr Freq Control. 2013; 60:281–289. [PubMed: 23357902]

Sorace AG, Warram JM, Umphrey H, Hoyt K. Microbubble-mediated ultrasonic techniques for improved chemotherapeutic delivery in cancer. J Drug Target. 2012; 20:43–54. [PubMed: 21981609]

Treat LH, McDannold N, Zhang Y, Vykhodtseva N, Hynynen K. Improved Anti-Tumor Effect of Liposomal Doxorubicin After Targeted Blood-Brain Barrier Disruption by MRI-Guided Focused Ultrasound in Rat Glioma. Ultrasound Med Biol. 2012; 38:1716–1725. [PubMed: 22818878]

Tucker ZC, Laguna BA, Moon E, Singhal S. Adjuvant immunotherapy for non-small cell lung cancer. Cancer Treat Rev. 2012; 38:650–661. [PubMed: 22226940]

Vermorken JB, Specenier P. Optimal treatment for recurrent/metastatic head and neck cancer. Ann Oncol. 2010; 21(Suppl 7):vii252–vii261. [PubMed: 20943624]

Zderic V, Vaezy S, Martin RW, Clark JI. Ocular drug delivery using 20-kHz ultrasound. Ultrasound Med Biol. 2002; 28:823–829. [PubMed: 12113795]

Zhao YZ, Dai DD, Lu CT, Lv HF, Zhang Y, Li X, Li WF, Wu Y, Jiang L, Li XK, Huang PT, Chen LJ, Lin M. Using acoustic cavitation to enhance chemotherapy of DOX liposomes: experiment in vitro and in vivo. Drug Dev Ind Pharm. 2012; 38:1090–1098. [PubMed: 22188116]

Zhao YZ, Lu CT, Zhou ZC, Jin Z, Zhang L, Sun CZ, Xu YY, Gao HS, Tian JL, Gao FH, Tang QQ, Li W, Xiang Q, Li XK, Li WF. Enhancing chemotherapeutic drug inhibition on tumor growth by ultrasound: an in vivo experiment. J Drug Target. 2011; 19:154–160. [PubMed: 20429773]

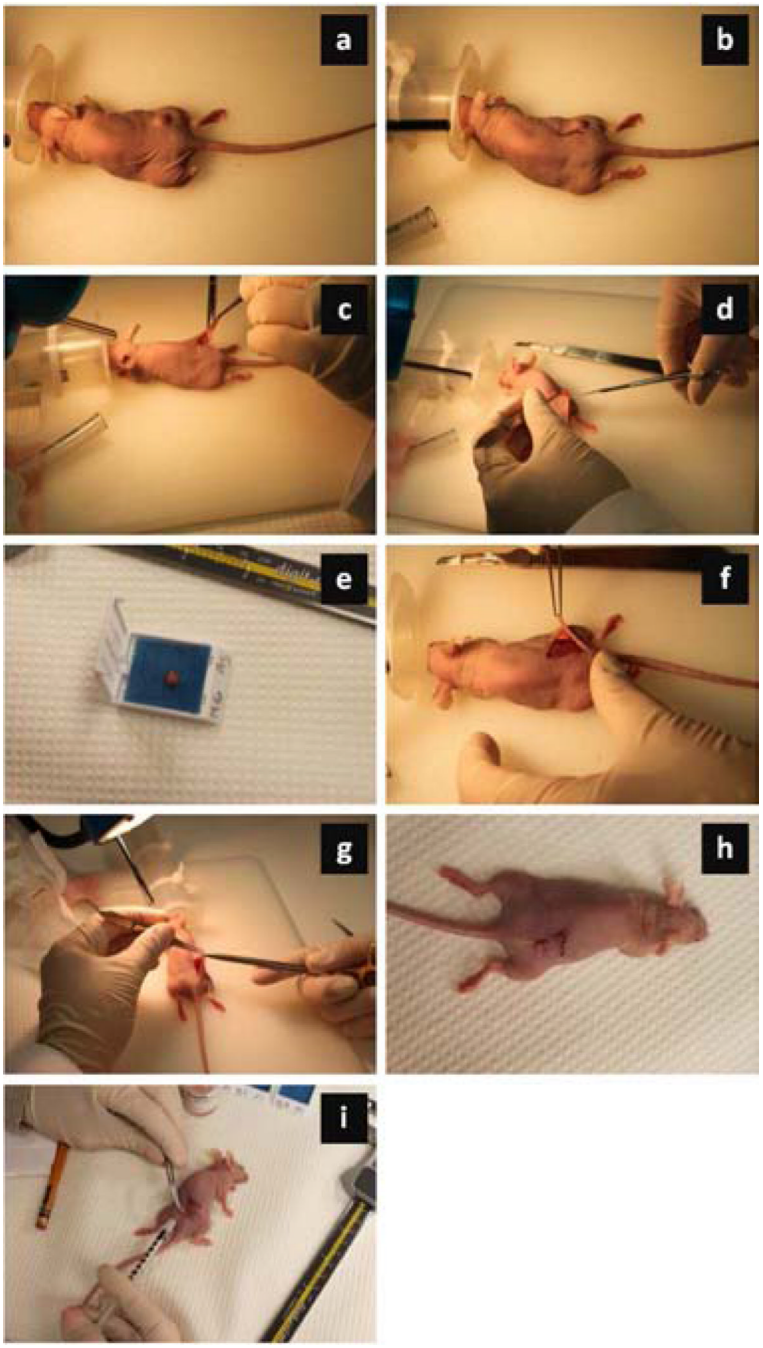

Figure 1.
Photograph series illustrating the surgical procedure for tumor removal and flap placement. Briefly, (a) each mouse was placed under general anesthesia with tumor located on the right flank. Then an (b) incision was made an estimated 1 cm from tumor in an “L” shape and the (c) flap was lifted. The (d) tumor was fully (or partially) resected and the (e) excised tumor sample was stored (shown is for 100% tumor resection group). Given the (f) wound bed with any residual (or remaining) tumorous tissue (0%), the (g) flap was sutured closed and the (h) anesthesia gas was discontinued. (i) Each mouse received a subcutaneous injection of pain medicine near the surgical site to minimize any discomfort from the surgical procedure.

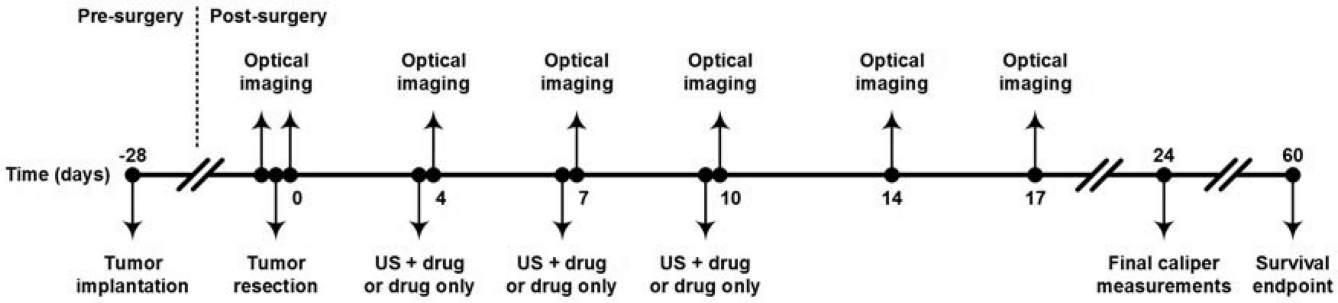

Figure 2.

Timeline for the experimental study detailing application of US-stimulated drug delivery (denoted US + drug) or drug only dosing in the adjuvant setting. Optical imaging techniques were used to monitor both drug delivery (fluorescence imaging) and treatment efficacy (bioluminescence imaging). Tumor size was recorded until day 24 and survival analysis was determined for 60 days post-surgical removal of tumor tissue.

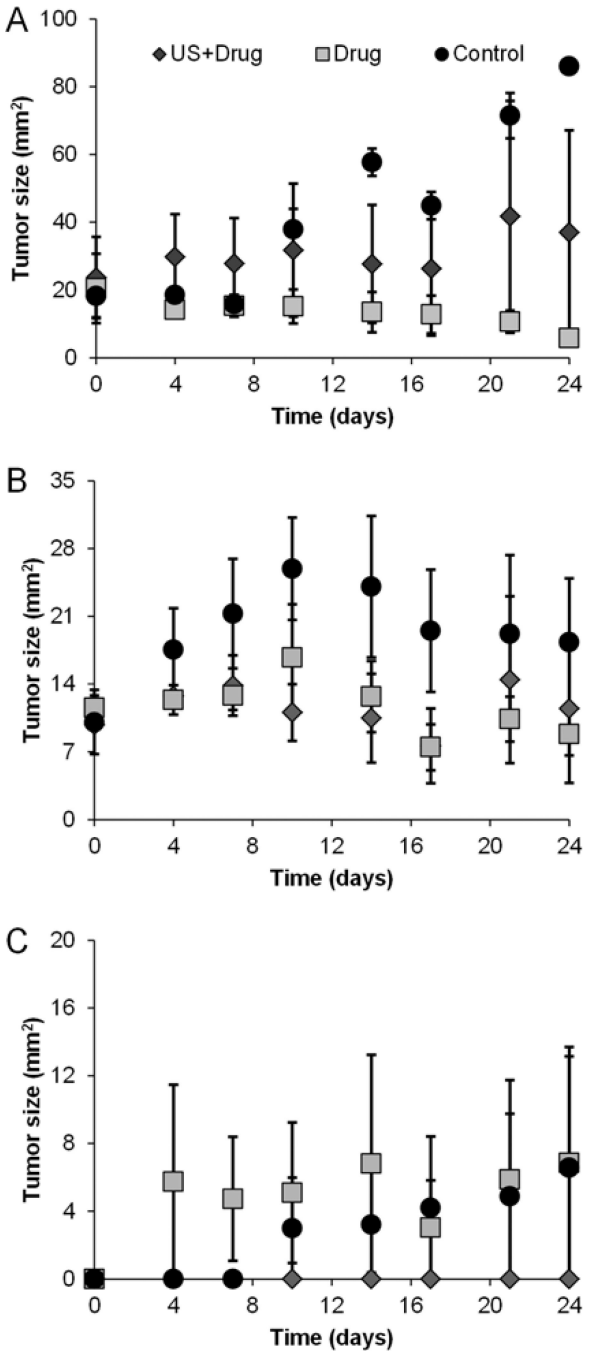

Figure 3.
Change in tumor size measurements performed biweekly until day 24 for each adjuvant therapeutic condition and animal group, namely, (a) 0% (b) 50%, or (c) 100% tumor resection.

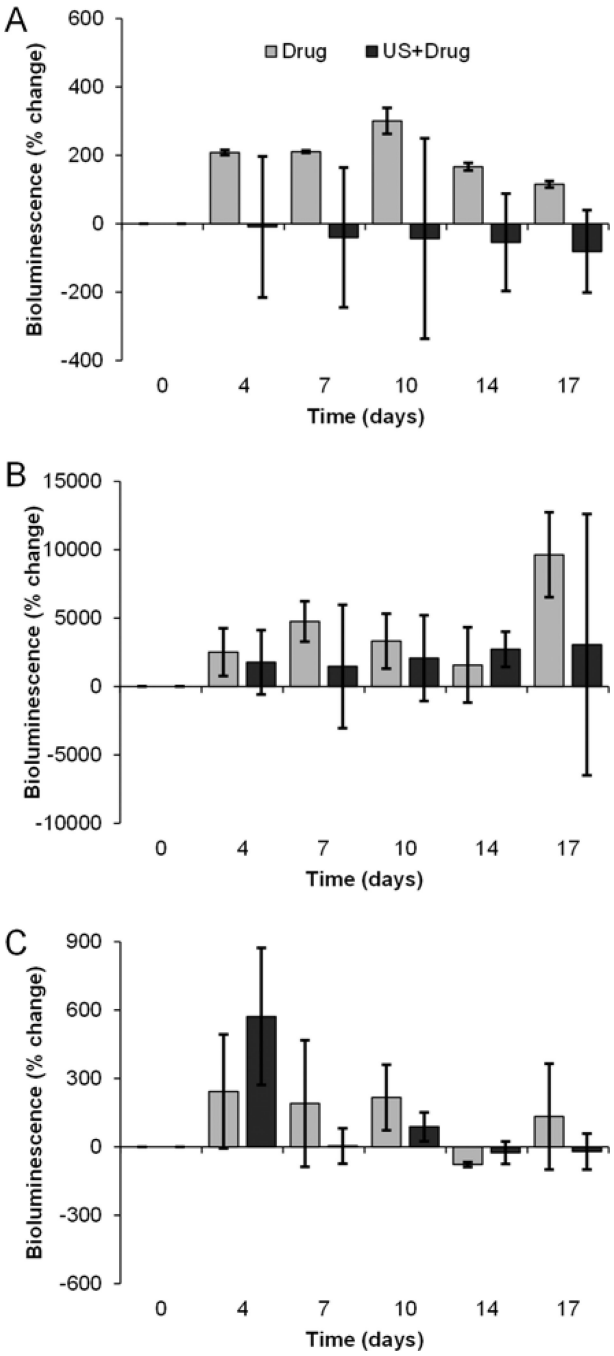

Figure 4.

Bioluminescence imaging of tumor viability after surgical resection. Bar graphs detail data acquired in the following animal groups, namely, (a) 0%, (b) 50% and (c) 100% tumor resection exposed to either US-stimulated drug delivery (denoted US + drug) or systemic drug treatment only. Note that animals treated with US-stimulated drug delivery exhibit improved anticancer effects (decreased tumor viability after surgical removal of tumor) in each group compared to drug alone.

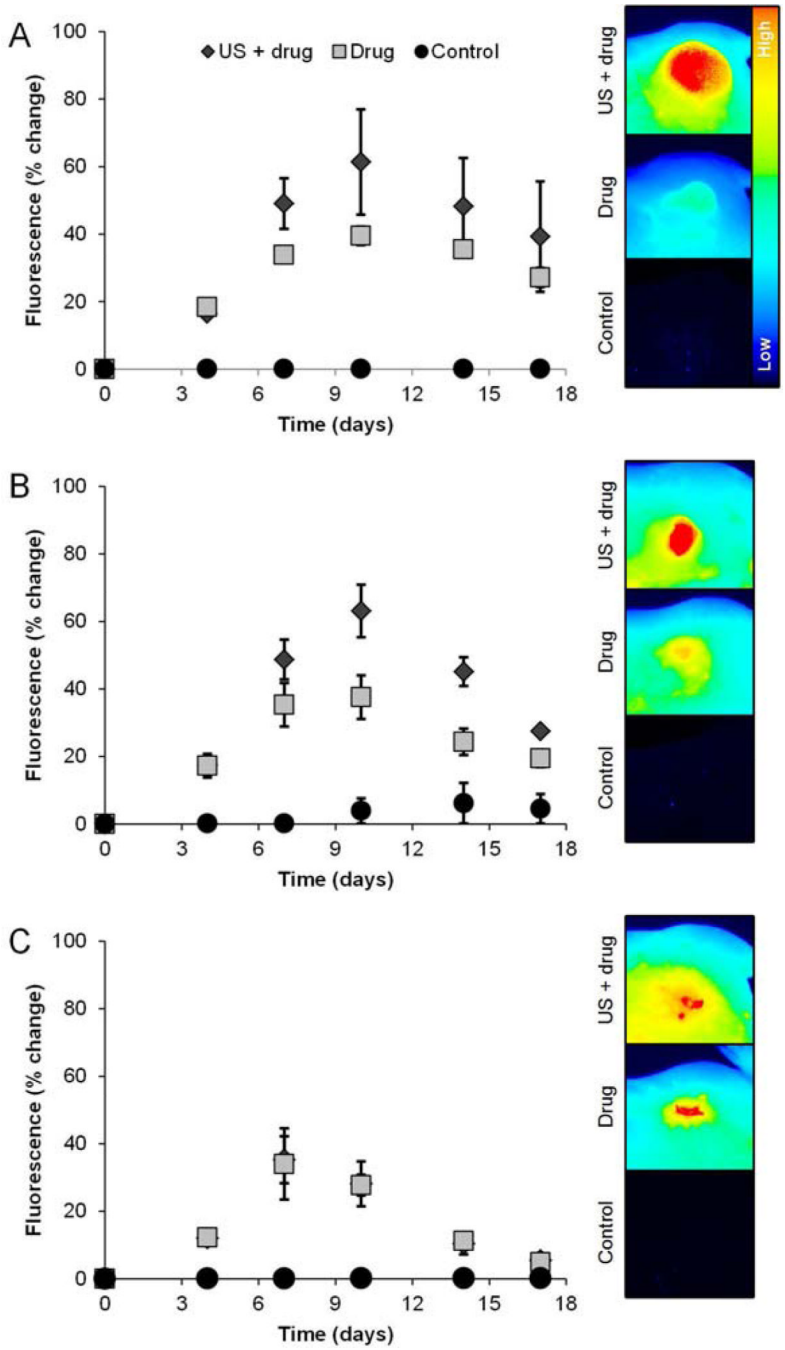

Figure 5.

Fluorescence imaging of drug uptake at the target tumor site. Line plots detail data acquired in the following animal groups, namely, (a) 0%, (b) 50% and (c) 100% tumor resection exposed to either US-stimulated drug delivery (denoted US + drug), systemic drug treatment alone, or sham (control) treatment (left). Note that animals treated with US-stimulated drug delivery tended to exhibit enhanced drug uptake compared to those dosed with drug only and control animals. Representative optical images of tumor fluorescence acquired on the last day of drug treatment (day 10 of the study) are presented and illustrate spatial distribution of drug accumulation in the target tumor (right).